Gadolinium-Based Nanoparticles Sensitize Ovarian Peritoneal Carcinomatosis to Targeted Radionuclide Therapy

Clara Diaz Garcia-Prada[1], Léna Carmes[2,3], Salima Atis[1], Ali Parach[1], Alejandro Bertolet[4], Marta Jarlier[5], Sophie Poty[1], Daniel Suarez Garcia[4], Wook-Geun Shin[4], Stanislas Du Manoir[1], Jan Schuemann[4], Olivier Tillement[2], François Lux[2,6], Julie Constanzo*[1], and Jean-Pierre Pouget*[1]

[1]*Institut de Recherche en Cancérologie de Montpellier, Inserm U1194, Université de Montpellier, Institut Régional du Cancer de Montpellier, Montpellier, France;* [2]*Institut Lumière Matière, Université Claude Bernard Lyon 1, Villeurbanne, France;* [3]*NH TherAguix S.A., Meylan, France;* [4]*Department of Radiation Oncology, Massachusetts General Hospital and Harvard Medical School, Boston, Massachusetts;* [5]*Biometrics Unit, Montpellier Cancer Institute, University of Montpellier, Montpellier, France; and* [6]*Institut Universitaire de France, Paris, France*

Ovarian cancer (OC) is the most lethal gynecologic malignancy (5-y overall survival rate, 46%). OC is generally detected when it has already spread to the peritoneal cavity (peritoneal carcinomatosis). This study investigated whether gadolinium-based nanoparticles (Gd-NPs) increase the efficacy of targeted radionuclide therapy using [^{177}Lu]Lu-DOTA-trastuzumab (an antibody against human epidermal growth factor receptor 2). Gd-NPs have radiosensitizing effects in conventional external-beam radiotherapy and have been tested in clinical phase II trials. **Methods:** First, the optimal activity of [^{177}Lu]Lu-DOTA-trastuzumab (10, 5, or 2.5 MBq) combined or not with 10 mg of Gd-NPs (single injection) was investigated in athymic mice bearing intraperitoneal OC cell (human epidermal growth factor receptor 2–positive) tumor xenografts. Next, the therapeutic efficacy and toxicity of 5 MBq of [^{177}Lu]Lu-DOTA-trastuzumab with Gd-NPs (3 administration regimens) were evaluated. NaCl, trastuzumab plus Gd-NPs, and [^{177}Lu]Lu-DOTA-trastuzumab alone were used as controls. Biodistribution and dosimetry were determined, and Monte Carlo simulation of energy deposits was performed. Lastly, Gd-NPs' subcellular localization and uptake, and the cytotoxic effects of the combination, were investigated in 3 cancer cell lines to obtain insights into the involved mechanisms. **Results:** The optimal [^{177}Lu]Lu-DOTA-trastuzumab activity when combined with Gd-NPs was 5 MBq. Moreover, compared with [^{177}Lu]Lu-DOTA-trastuzumab alone, the strongest therapeutic efficacy (tumor mass reduction) was obtained with 2 injections of 5 mg of Gd-NPs/d (separated by 6 h) at 24 and 72 h after injection of 5 MBq of [^{177}Lu]Lu-DOTA-trastuzumab. In vitro experiments showed that Gd-NPs colocalized with lysosomes and that their radiosensitizing effect was mediated by oxidative stress and inhibited by deferiprone, an iron chelator. Exposure of Gd-NPs to ^{177}Lu increased the Auger electron yield but not the absorbed dose. **Conclusion:** Targeted radionuclide therapy can be combined with Gd-NPs to increase the therapeutic effect and reduce the injected activities. As Gd-NPs are already used in the clinic, this combination could be a new therapeutic approach for patients with ovarian peritoneal carcinomatosis.

Key Words: radiosensitization; radiopharmaceutical; radioimmunotherapy; TRT; ovarian cancer; Auger electrons

J Nucl Med 2023; 64:1956–1964
DOI: 10.2967/jnumed.123.265418

Ovarian cancer (OC) is the most lethal gynecologic malignancy, the fifth most common cancer type, and the fourth most common cause of cancer-related death worldwide (*1,2*). Cytoreductive surgery and platinum-based chemotherapy are the standard therapy for newly diagnosed advanced OC (*2,3*). However, approximately 70% of patients will relapse in the next 3 y (*2*). Recurrent OC can spread into the peritoneal cavity, known as peritoneal carcinomatosis (PC) (*4*). Bevacizumab (*5,6*) is used for first-line chemotherapy and maintenance treatment of some of these patients. Inhibitors of the DNA repair enzyme poly-(adenosine diphosphate ribose) polymerase 1 (*4,6*) also are proposed for maintenance treatment of patients with advanced OC with BRCA mutations (*7*). New antibody-based strategies against immune checkpoint inhibitors (NCT05188781), tumor-associated cancer antigen 125 (NCT04498117), folate receptor α (NCT05200364), mesothelin (NCT0537269), the sodium-dependent phosphate transporter NaPi2b (NCT04907968), and Müllerian hormone type II receptor (NCT02978755) (*8,9*) are being investigated. Targeted radionuclide therapy (TRT) (*10,11*), using monoclonal antibodies or their fragments radiolabeled with β, α, or Auger emitters, has been assessed in preclinical models (*12–22*) and clinical trials (*23–28*). TRT is a particularly attractive alternative for the management of diffuse and small-volume tumor nodules, such as those remaining after surgery of PC from OC (OC-PC), because it specifically targets and irradiates tumor cells (*29*). Moreover, the use of radionuclides emitting high linear energy transfer (LET) particles, such as α or Auger electrons, could at least theoretically overcome OC cell radioresistance, which is one of the limitation of β-TRT for solid tumors. However, clinical TRT of OC-PC using high LET particles is still being evaluated (NCT03732768) (*30–33*).

Here, we propose a new approach to improve TRT efficacy in OC-PC. The rationale is to combine TRT with gadolinium-based nanoparticles (Gd-NPs) (NH TherAguix). Gd-NPs are smaller than 5 nm and made of a polysiloxane matrix on which gadolinium chelates are covalently grafted. Once in the bloodstream, Gd-NPs diffuse into tumors according to the enhanced permeability and retention effect, as demonstrated in many preclinical models (*34*).

Received Jan. 10, 2023; revision accepted Aug. 28, 2023.
For correspondence or reprints, contact Jean-Pierre Pouget (jean-pierre.pouget@inserm.fr) or Julie Constanzo (julie.constanzo@inserm.fr).
*Contributed equally to this work.
Published online Oct. 19, 2023.

Besides their contrast agent properties for MRI, Gd-NPs are one of the few nanodrugs that have been translated into the clinic for theranostic applications (*34–36*). Gd-NPs showed an enhanced therapeutic effect in vivo after conventional external beam radiotherapy (EBRT) in different tumor models, including radioresistant cancers (*34*). Several hypotheses have been proposed to explain this effect. First, Gd-NPs increase the probability of interactions with photons (or β-particles) as Gd-NPs introduce a high atomic number material in tumors, leading to a local increase in absorbed dose. Second, Auger electron cascades are generated when gadolinium electronic shells reorganize after 1 electron is ejected on irradiation. These Auger electron cascades are responsible for the high localized energy deposition that drastically damages cells if near a subcellular radiosensitive target. The aim of this proof-of-concept study was to demonstrate that TRT using [^{177}Lu]Lu-DOTA-trastuzumab combined with Gd-NPs is a new therapeutic avenue for patients with OC-PC.

MATERIALS AND METHODS

The human SK-OV-3 and OVCAR-3 (high-grade serous OC) and A-431 (vulvar epidermal carcinoma) cell lines were from the American Type Culture Collection. The monoclonal antibody trastuzumab was chosen because it targets human epidermal growth factor receptor 2 expressed by these cell lines (*37*).

More information on the cell lines is available in the supplemental materials (available at http://jnm.snmjournals.org), which also describe establishment of an OC-PC model in athymic female Swiss nude mice, calibration of the bioluminescence signal intensity as a function of tumor mass, radiolabeling of trastuzumab and Gd-NPs (*38–41*), the mouse treatments, SPECT/CT imaging of [^{111}In]In-Gd-NPs, the biodistribution of [^{111}In]In-DTPA-trastuzumab and Gd-NPs, cell localization and uptake of Gd-NPs, clonogenic cell survival (*42–45*), assessment of the role of oxidative stress and of deferiprone in the radiosensitizing effects of Gd-NPs, the Monte Carlo simulations and dosimetry (*46–48*), and the statistical analysis.

RESULTS

Calibration of Bioluminescence Signal and Determination of Experimental Endpoint

First, the calibration curve for the bioluminescence signal as a function of the tumor mass was established to monitor tumor growth (Supplemental Fig. 1A), determine the time at which treatment should start, and determine the time at which mice bearing SK-OV-3-luc cell xenografts should be euthanized (OC-PC model). The total tumor mass was about 15.0 mg per mouse (divided into 4–8 nodules) at treatment initiation (day 15 after xenograft). In the following experiments, all mice were euthanized when the bioluminescence signal reached 4×10^{10} photons/s. which corresponded to a total tumor mass of about 2,000 mg (Supplemental Fig. 1A).

Gd-NP and [^{177}Lu]Lu-DOTA-Trastuzumab Biodistribution in Mice

The biodistribution study on mice with SK-OV-3-luc cell xenografts indicated that uptake of [^{111}In]In-DTPA-trastuzumab in tumors maximized between 24 and 72 h after injection and peaked at 48 h (71.5% ± 7.7% injected activity/g) (Fig. 1, left). In blood, uptake peaked at 24 h (17.9% ± 2.4% injected activity/g) and decreased progressively to reach 17.9% ± 2.4% injected activity/g at 168 h after injection. Conversely, uptake of Gd-NPs in tumors maximized at 30 min after injection (4,267 ± 80 mmol/g) and decreased to 804 ± 321 mmol/g at 6 h (Fig. 1, middle). Gd-NPs strongly accumulated in the kidneys (5,138 ± 317 mmol/g) at 6 h after injection, suggesting its renal elimination. SPECT/CT imaging of mice after intraperitoneal injection of [^{111}In]In-Gd-NPs confirmed the tumor uptake and renal excretion (Supplemental Fig. 1B). Moreover, ex vivo dual-isotope SPECT/CT imaging confirmed [^{177}Lu]Lu-Gd-NPs and [^{125}I]I-trastuzumab colocalization in tumor nodules collected from mice (Fig. 1, right). Therefore, for testing the combination, animals received 1 injection of [^{177}Lu]Lu-DOTA-trastuzumab followed 48 h later by Gd-NPs.

Optimal [^{177}Lu]Lu-DOTA-Trastuzumab Activity for Combination with Gd-NPs

In this first set of experiments to evaluate the combination of [^{177}Lu]Lu-DOTA-trastuzumab plus Gd-NPs (optimal activity study, Supplemental Table 1), mice were euthanized at week 4 after treatment. This time point was when the first mouse in the NaCl-treated group reached the tumor mass limit. Tumors were collected and their size measured and weight calculated to assess the treatment efficacy.

Tumor mass was significantly reduced in mice treated with 50 μg of trastuzumab plus 10 mg of Gd-NPs compared with the NaCl-treated group ($P = 0.0150$) (Fig. 2A). This might be explained by the trastuzumab effect. In mice treated with [^{177}Lu]Lu-DOTA-trastuzumab at the maximum tolerated activity (10 MBq, previously determined by

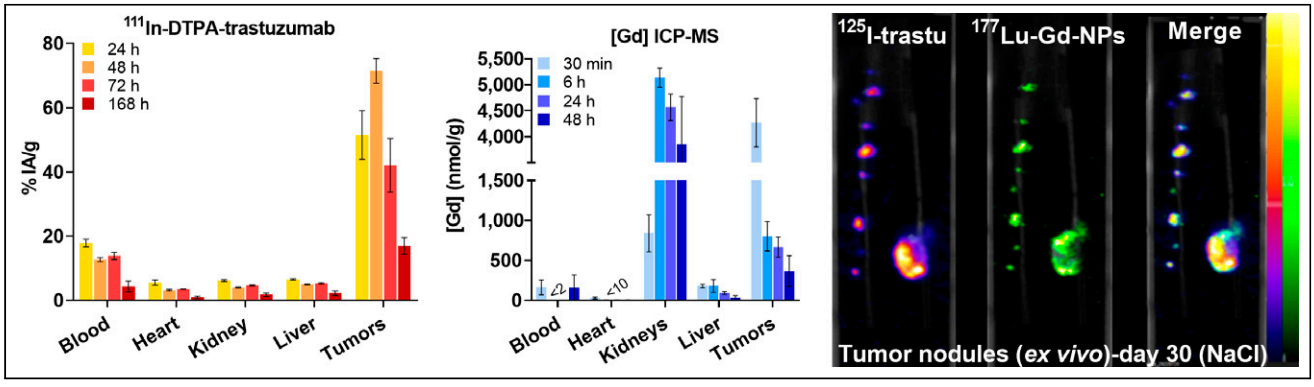

FIGURE 1. (Left) Biodistribution of [^{111}In]In-DTPA-trastuzumab determined by ex vivo γ-counting of tumor nodules and organs collected at various times (4 per time point) after intraperitoneal injection. (Middle) Biodistribution of Gd-NPs by inductively coupled plasma mass spectrometry in tumor nodules and organs collected at various times after intraperitoneal injection (3 per time point). Results are mean ± SEM. (Right) Ex vivo SPECT/CT dual-isotope imaging of SK-OV-3-luc cell tumors collected from mice after intraperitoneal injection of [^{125}I]I-trastuzumab and [^{177}Lu]Lu-CuPRiX (NH TherAguix S.A. and Institut Lumière Matière) Gd-NPs. Merged images confirmed colocalization of trastuzumab and CuPRiX NPs. % IA = percentage injected activity; DTPA = diethylenetriaminepentaacetic acid; ICP-MS = inductively coupled plasma mass spectrometry; trastu = trastuzumab.

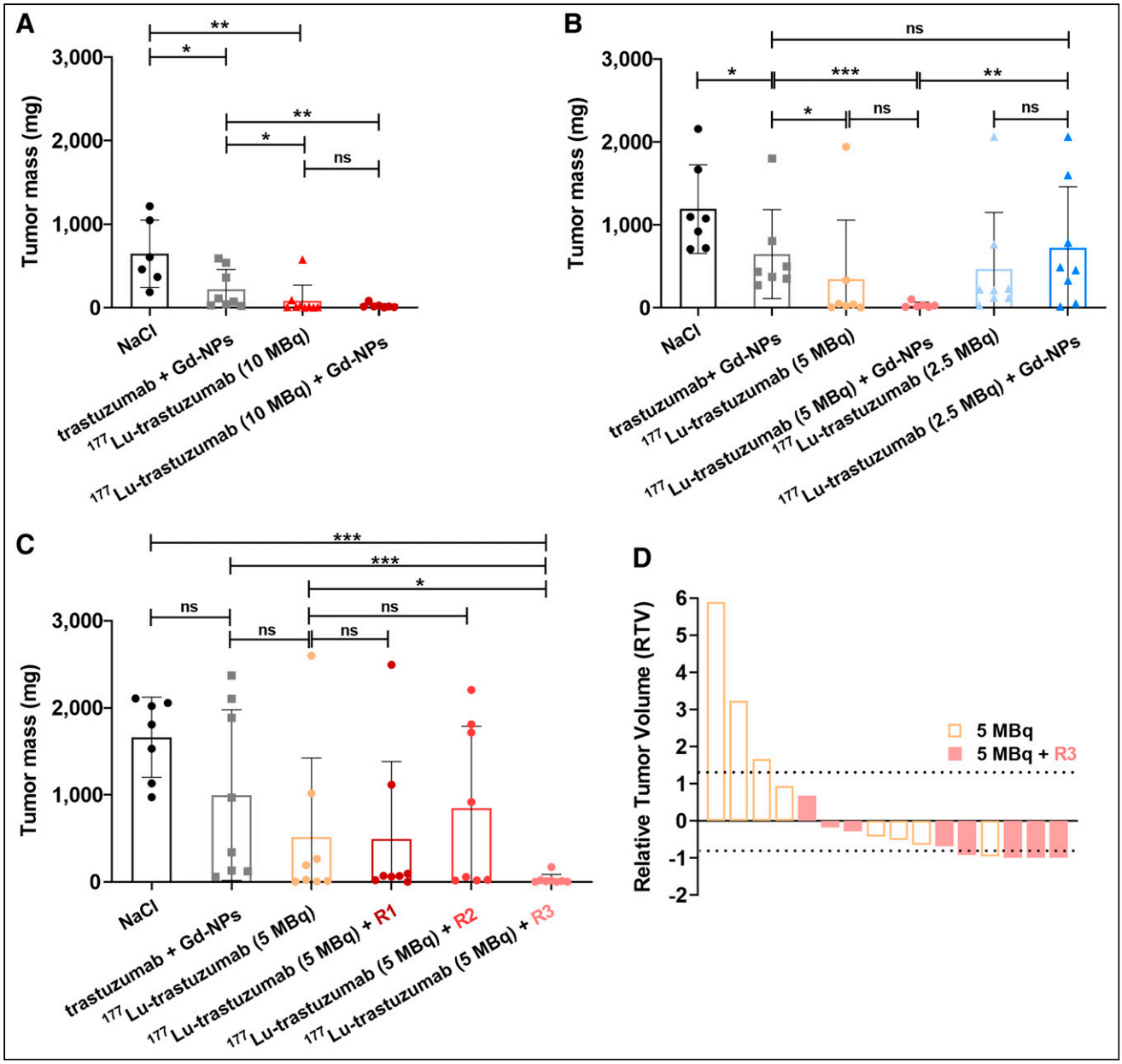

FIGURE 2. Determination of therapeutic efficacy of [^{177}Lu]Lu-DOTA-trastuzumab combined with Gd-NPs. (A and B) Tumor mass was determined in mice treated with maximum tolerated activity (10 MBq) of [^{177}Lu]Lu-DOTA-trastuzumab followed or not (48 h later) by 10 mg of Gd-NPs (A) and low (2.5 MBq) or intermediate (5 MBq) activity of [^{177}Lu]Lu-DOTA-trastuzumab followed or not (48 h later) by 10 mg of Gd-NPs (B). (C) Tumor mass in mice treated with 5 MBq of [^{177}Lu]Lu-DOTA-trastuzumab regimen 1 (1 injection of 4 mg of Gd-NPs/d for 5 d starting 48 h after [^{177}Lu]Lu-DOTA-trastuzumab injection), regimen 2 (2 injections of 2 mg of Gd-NPs/d for 5 d starting 48 h after [^{177}Lu]Lu-DOTA-trastuzumab), or regimen 3 (2 injections of 5 mg of Gd-NPs per day at 24 and 72 h after [^{177}Lu]Lu-DOTA-trastuzumab). (D) Relative tumor volume at treatment end. Results are mean ± SD. *$P < 0.05$. **$P < 0.01$. ***$P < 0.001$. ns = not significant (Mann–Whitney *t* test).

TABLE 1
Number of Mice with Objective Response, Stable Disease, and Progressive Disease at Week 4 After Treatment

Outcome	[^{177}Lu]Lu-DOTA-trastuzumab (10 MBq) (n = 9)	[^{177}Lu]Lu-DOTA-trastuzumab (5 MBq) (n = 8)	[^{177}Lu]Lu-DOTA-trastuzumab (5 MBq) + regimen 3 (n = 8)
Objective response	5	1	5
Stable disease	1	4	3
Progressive disease	3	3	0

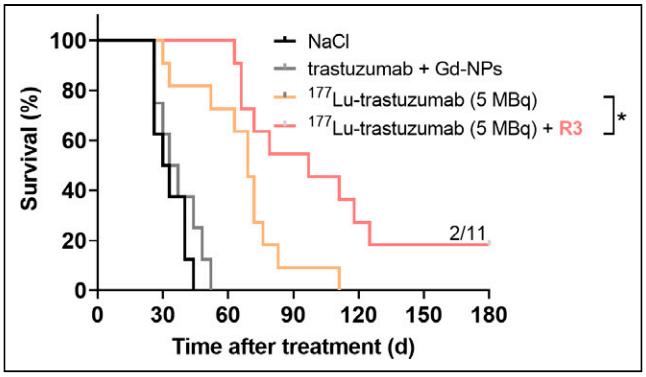

FIGURE 3. Kaplan–Meier survival analysis of mice bearing intraperitoneal SK-OV-3-luc tumor cell xenografts. Mice received single intraperitoneal injection of NaCl, 25 μg of trastuzumab plus Gd-NPs (2 × 5 mg per day, 24 and 72 h after trastuzumab), 5 MBq of [^{177}Lu]Lu-DOTA-trastuzumab, or 5 MBq of [^{177}Lu]Lu-DOTA-trastuzumab plus Gd-NPs (2 × 5 mg per day, 24 and 72 h after TRT). R3 = regimen 3.

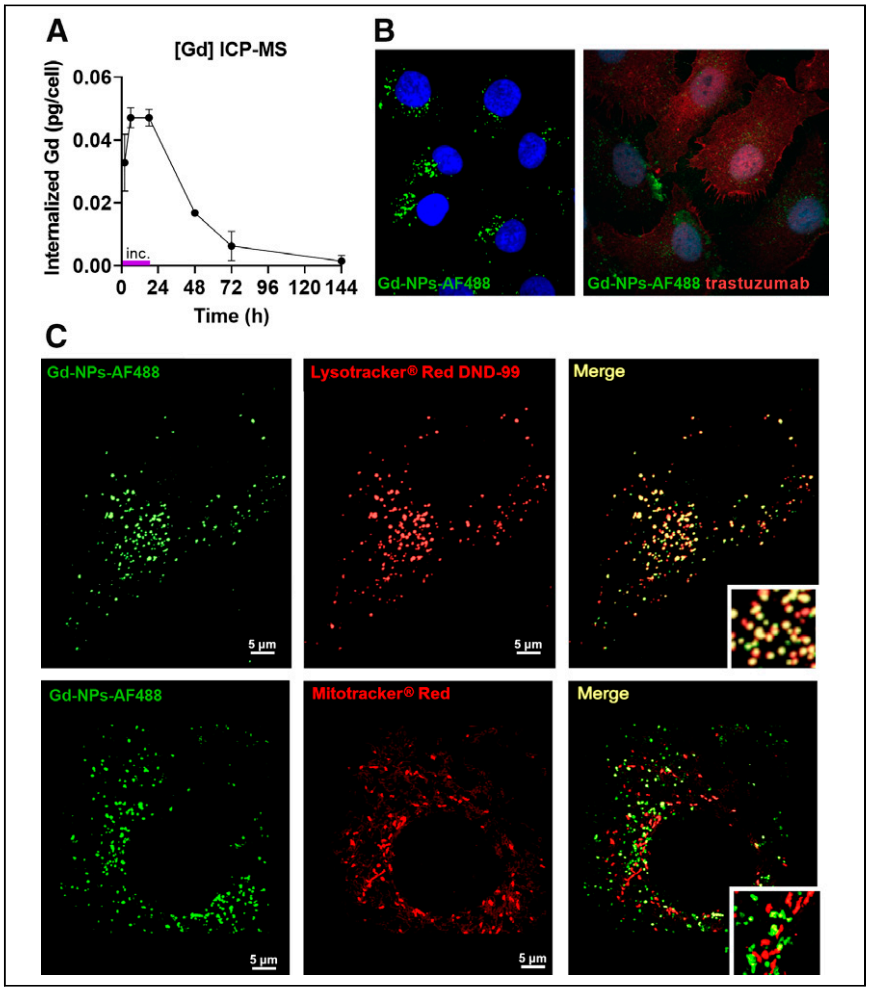

FIGURE 4. Gd-NP uptake and subcellular localization. (A) Cellular uptake was measured in SK-OV-3-luc cells by inductively coupled plasma mass spectrometry after 18 h of incubation with Gd-NPs, 10 mg/mL. Results are mean ± SD of 3 independent experiments performed in triplicate. (B) Cytoplasmic localization of Gd-NP Alexa Fluor 488 (Life Technologies Corp.) (left) and trastuzumab (right) by immunofluorescence analysis. (C) Colocalization of Gd-NP Alexa Fluor 488 with lysosomes (Lysotracker red DND-99; Molecular Probes, Inc.) but not with mitochondria (Mitotracker red CMXRos; Molecular Probes, Inc.). ICP-MS = inductively coupled plasma mass spectrometry.

our group [unpublished data, October 2022]), tumor mass was significantly decreased at week 4 after injection compared with the NaCl-treated group (P = 0.0014). Tumor mass in the group receiving [^{177}Lu]Lu-DOTA-trastuzumab plus 10 mg of Gd-NPs was significantly decreased compared with the group receiving trastuzumab plus Gd-NPs (P = 0.0030) (Fig. 2A). This result highlighted the additional therapeutic effect of ^{177}Lu irradiation. However, addition of Gd-NPs did not significantly increase [^{177}Lu]Lu-DOTA-trastuzumab efficacy (P = 0.3788) (Fig. 2A). On the basis of these results, 10 MBq of [^{177}Lu]Lu-DOTA-trastuzumab was considered too efficient to observe any additional benefit of the combination of Gd-NPs plus [^{177}Lu]Lu-DOTA-trastuzumab. Therefore, in a second experiment (Fig. 2B), [^{177}Lu]Lu-DOTA-trastuzumab activity was decreased to 5 MBq. Tumor mass was significantly lower in the [^{177}Lu]Lu-trastuzumab group than in the trastuzumab plus Gd-NPs group (343 vs. 648 mg, P = 0.0189), indicating that 5 MBq was still a therapeutic activity (Fig. 2B). Tumor mass was even lower in the trastuzumab plus Gd-NPs group (34 vs. 648 mg, P = 0.0012). However, the difference between [^{177}Lu]Lu-DOTA-trastuzumab and [^{177}Lu]Lu-trastuzumab plus Gd-NPs was not significant (P = 0.3141) (Fig. 2B). Therefore, [^{177}Lu]Lu-DOTA-trastuzumab activity was decreased to 2.5 MBq. In this case, tumor mass did not differ among the groups receiving [^{177}Lu]Lu-DOTA-trastuzumab, [^{177}Lu]Lu-DOTA-trastuzumab plus Gd-NPs, and trastuzumab plus Gd-NP (470 vs. 723 mg, P = 0.1989) (Fig. 2B). This finding indicated that 2.5 MBq was too low to observe any additional therapeutic effect of ^{177}Lu irradiation. In addition, the mean tumor mass in the group receiving 2.5 MBq of [^{177}Lu]Lu-DOTA-trastuzumab plus Gd-NPs was higher than in the group receiving 5 MBq of [^{177}Lu]Lu-DOTA-trastuzumab plus Gd-NPs (P = 0.0040).

Therefore, 5 MBq was selected as the optimal injected activity because it showed a good compromise between efficacy and a possible Gd-NP–mediated radiosensitizing effect.

Improvement of TRT Efficacy Through Gd-NP Fractionated Administration

The next step (fractionation regimen study, Supplemental Table 1) was to investigate whether Gd-NPs fractionated administration could improve therapeutic efficacy. As previously performed, mice were euthanized at week 4 after xenograft, tumors were collected, and tumor mass was determined. Fractionation allowed increasing the Gd-NP injected mass to 20 mg, which is the maximum tolerated dose in mice (*31*). [^{177}Lu]Lu-DOTA-trastuzumab (5 MBq) was combined with Gd-NPs administered according to the 3 different regimens described in the Materials and Methods. Regimen 3 (5 MBq [^{177}Lu]Lu-DOTA-trastuzumab + Gd-NPs, 2 × 5 mg per day, 24 and 72 h after TRT) showed the strongest effect on tumor mass (P = 0.0320)

TABLE 2
Gd-NP Number in Lysosomes as Function of Time, According to Cellular Uptake Measurements

Gd-NP	2 h	6 h	18 h	48 h	72 h	144 h
Number	258.007	369.983	370.171	132.129	49.465	11.573

compared with [^{177}Lu]Lu-DOTA-trastuzumab alone (Fig. 2C). According to the relative tumor volume criteria (Supplemental Fig. 2; Table 1), in the [^{177}Lu]Lu-DOTA-trastuzumab plus regimen 3 group (8 mice), 5 mice had an objective response and no mouse showed progressive disease. In the [^{177}Lu]Lu-DOTA-trastuzumab group (8 mice), only 1 mouse showed an objective response, 3 mice had progressive disease, and 4 had stable disease. Although efficacy was good in the 10-MBq treatment group (9 mice; optimal activity study, Supplemental Table 1), 3 mice still had progressive disease and only 5 objective responses were observed. In addition, no difference in bone marrow toxicity or weight loss was observed between the group receiving 5 MBq of [^{177}Lu]Lu-DOTA-trastuzumab and the group receiving 5 MBq of [^{177}Lu]Lu-DOTA-trastuzumab plus regimen 3 (Supplemental Figs. 3–4).

Kaplan–Meyer survival curves were established (survival study, Supplemental Table 1) and confirmed that regimen 3 led to the strongest improvement in median survival (Fig. 3A). Specifically, [^{177}Lu]Lu-DOTA-trastuzumab plus regimen 3 led to a significant increase in survival (median survival, 97 d, with 2/11 mice cured) compared with NaCl (median survival, 30 d; $P < 0.0001$), trastuzumab plus Gd-NPs (median survival, 33 d; $P < 0.0001$), and 5 MBq of [^{177}Lu]Lu-DOTA-trastuzumab alone (median survival, 69 d; $P = 0.016$). The relative tumor volume data as a function of time are shown in Supplemental Fig. 4.

Mean Organ- and Tumor-Absorbed Doses

The mean tumor-absorbed dose on injection of 5 MBq of [^{177}Lu]Lu-DOTA-trastuzumab was 1.99 ± 0.21 Gy, whereas it was less than 0.5 Gy for normal tissues, except for blood (0.570 ± 0.002 Gy) (Supplemental Fig. 5). These data were used to assess whether Gd-NPs contributed to the absorbed dose enhancement.

Gd-NPs Radiosensitization of Tumor Cells to [^{177}Lu]Lu-DOTA-Trastuzumab In Vitro

To understand the in vivo Gd-NP–mediated radiosensitizing effect, Gd-NP (10 mg/mL) cellular uptake was monitored in SK-OV-3-luc cells at different time points after incubation (from 2 to 144 h) (Fig. 4A; Table 2). Uptake plateaued from 6 to 18 h (0.047 ± 0.003 pg/cell) before decreasing slowly when culture medium with Gd-NPs was removed and cells were washed. Both Gd-NPs (Fig. 4B, left) and trastuzumab (Fig. 4B, right) were detected in the cytoplasm but not in the cell nucleus. Gd-NPs colocalized with lysosomes but not with mitochondria (Fig. 4C).

In addition, [^{177}Lu]Lu-DOTA-trastuzumab uptake peaked at 18 h (0.045 ± 0.007 Bq/cell) before progressively decreasing (Fig. 5A). Analysis of clonogenic survival of SK-OV-3-luc, A-431, and OVCAR-3 cells exposed to [^{177}Lu]Lu-DOTA-trastuzumab (at different test activities) with or without Gd-NPs, 10 mg/mL (Fig. 5B; Supplemental Fig. 6; Table 3), showed the radiosensitizing effect of Gd-NPs. In the presence of Gd-NPs, the same cytotoxic effect was obtained with half the tested volume activity (MBq/mL). For example, in all 3 cell lines, the combination of [^{177}Lu]Lu-DOTA-trastuzumab, 1 MBq/mL, plus Gd-NPs was as cytotoxic as [^{177}Lu]Lu-DOTA-trastuzumab, 2 MBq/mL, alone. Gd-NPs alone did not induce any significant cytotoxic effect in the 3 cell lines (survival fraction > 87%) (Supplemental Fig. 7). The Bliss independence mathematic model confirmed the synergistic effect between Gd-NPs and [^{177}Lu]Lu-DOTA-trastuzumab. The predicted and observed survival fractions used in the Bliss model are listed in Table 3. In addition, radiosensitizing effect values of more than 1 indicate the radiosensitizing effect of Gd-NPs (Table 3).

The role of oxidative stress in Gd-NPs in radiosensitizing effect was demonstrated using *N*-acetyl-L-cysteine, catalase, and dimethyl sulfoxide (Fig. 6A). Indeed, when SK-OV-3-luc cells were coincubated with Gd-NPs and each of these antioxidants, clonogenic survival was increased. These results were confirmed using deferiprone, an iron chelator that prevents reactive oxygen species formation (Fig. 6B).

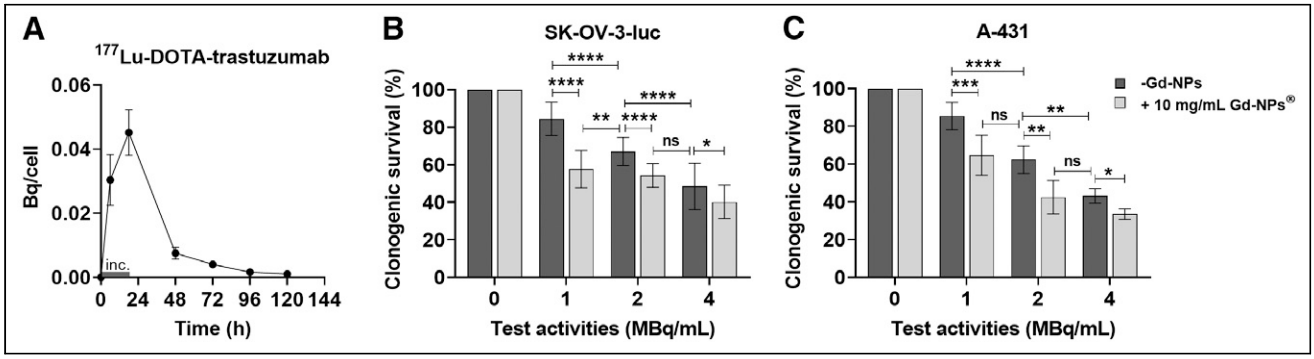

FIGURE 5. [^{177}Lu]Lu-DOTA-trastuzumab uptake and cytotoxic effects when combined with Gd-NPs. (A) [^{177}Lu]Lu-DOTA-trastuzumab uptake in SK-OV-3-luc cells incubated with radiolabeled antibody, 1 MBq/mL, for 18 h. (B and C) Clonogenic survival of SK-OV-3-luc (B) and A-431 (C) cells incubated with [^{177}Lu]Lu-DOTA-trastuzumab (0–4 MBq/mL) with or without Gd-NPs, 10 mg/mL, for 18 h. Results are mean ± SD of 3 independent experiments performed in triplicate. Role of oxidative stress in Gd-NP radiosensitizing effect was demonstrated using *N*-acetyl-L-cysteine, catalase, and dimethyl sulfoxide (Fig. 6A). Indeed, when SK-OV-3-luc cells were coincubated with Gd-NPs and each of these antioxidants, clonogenic survival increased. These results were confirmed using deferiprone, an iron chelator that prevents reactive oxygen species formation (Fig. 6B). *$P < 0.05$. **$P < 0.01$. ***$P < 0.001$. ****$P < 0.0001$. inc = incubation time (18 h); ns = not significant (Mann–Whitney *t* test).

TABLE 3
Survival Fraction and Radiosensitizing Effect of TRT With or Without Gd-NPs (10 mg/mL) in Different Cell Lines

Cell line	Survival fraction (%)								Radiosensitizing effect		
	1 MBq/mL	1 MBq/mL + Gd-NPs	Predicted*	2 MBq/mL	2 MBq/mL + Gd-NPs	Predicted*	4 MBq/mL	4 MBq/mL + Gd-NPs	Predicted*	1 MBq/mL	2 MBq/mL	4 MBq/mL
SK-OV-3-luc	84.4 ± 8.8	57.6 ± 9.9	70.9	67.0 ± 7.5	54.3 ± 6.3	54.3	48.5 ± 12.4	40.2 ± 8.9	35.9	1.46	1.23	1.20
A-431	85.4 ± 7.3	64.6 ± 10.7	74.8	62.3 ± 7.3	42.4 ± 8.9	54.6	43.1 ± 3.8	33.5 ± 2.8	37.8	1.32	1.59	1.28
OVCAR-3	82.3 ± 10.5	60.8 ± 10.1	72.1	60.4 ± 10.1	42.8 ± 11.6	52.9	37.5 ± 10.6	30.4 ± 9.9	32.9	1.35	1.41	1.23

*Values based on Bliss independence model.

Generation of Auger Electrons Through Gd-NP Exposure to [^{177}Lu]Lu-DOTA-Trastuzumab

Monte Carlo simulations were used to investigate the interactions between ^{177}Lu atoms and lysosomes in the presence and absence of Gd-NPs. The simulations included 2 steps (Supplemental Fig. 8). In the first step, ^{177}Lu atoms were distributed within a cell (i.e., postincubation scenario) or in the 1-mm-diameter medium surrounding the cell (i.e., incubation scenario in the presence of extracellular medium). ^{177}Lu atoms underwent radioactive decay, and particles that reached a lysosome were stored in a phase space file. In the second step, particles from the phase space were simulated in lysosomes with a variable number of Gd-NPs distributed uniformly, according to the results of the Gd-NP uptake assay. Supplemental Fig. 8B shows the continuous energy spectrum (0–498 keV) of electrons emitted by ^{177}Lu that reached the lysosomes in the incubation scenario after the first simulation step. A peak at around 100 keV that corresponded to conversion electrons was also observed. Figure 7 displays the dose rates and accumulated doses in lysosomes at various time points in the incubation (18 h) and postincubation scenarios. The dose rates were calculated for each time point, and the accumulated doses were calculated as a trapezoidal integral of the obtained curves. The incubation scenario took into account radioactive decay at each time point, whereas the postincubation scenario used the activity measured in the [^{177}Lu]Lu-DOTA-trastuzumab uptake assays. Results were similar in the presence and absence of Gd-NPs, indicating that Gd-NPs did not increase the absorbed dose. Moreover, the contribution of photoelectrons was extremely low (about 10^{-4} photoelectric events) (Supplemental Fig. 8C). On the other hand, the Auger electron production rate and cumulative number in lysosomes in the same conditions and scenarios were increased in the presence of Gd-NPs (Fig. 7).

DISCUSSION

In this study, we assessed a novel therapeutic combination ([^{177}Lu]Lu-DOTA-trastuzumab and Gd-NPs) for OC-PC. The combination of EBRT plus Gd-NPs is being evaluated in phase II clinical trials to treat brain metastases by whole-brain irradiation (NCT03818386) and stereotactic irradiation (NCT04899908), in phase I/II clinical trials to treat glioblastoma in combination with temozolomide and radiotherapy (NCT04881032), and in phase I/II trials to treat pancreatic and lung tumors by MRI-LINAC (NCT04789486). Gd-NPs are intravenously injected at an optimized time before EBRT. Therefore, we first identified the optimized conditions for TRT ([^{177}Lu]Lu-DOTA-trastuzumab activity) with Gd-NPs (dose and fractionation regimen) in a mouse model of OC-PC. We found that 1 injection of 5 mg of Gd-NPs twice per day 24 and 72 h after 5 MBq of [^{177}Lu]Lu-DOTA-trastuzumab (Supplemental Table 1) was required to maximize the combination effect. Tumor mass was significantly different after injection of 5 MBq of [^{177}Lu]Lu-DOTA-trastuzumab with and without Gd-NPs ($P = 0.032$).

The more restrictive P value (i.e., $P = 0.01$, compared with 0.05 used in this study) required for pairwise comparisons would result in a loss of statistical significance. However, these results at day 30 were confirmed by the survival experiments, since the latter showed that tumors treated with the combination were always smaller, over the 130-d period considered, than were tumors treated with [^{177}Lu]Lu-DOTA-trastuzumab alone. For example, tumor volume on day 36 ($P = 0.0078$) and day 42 ($P = 0.0078$), which are comparable time points, was statistically different.

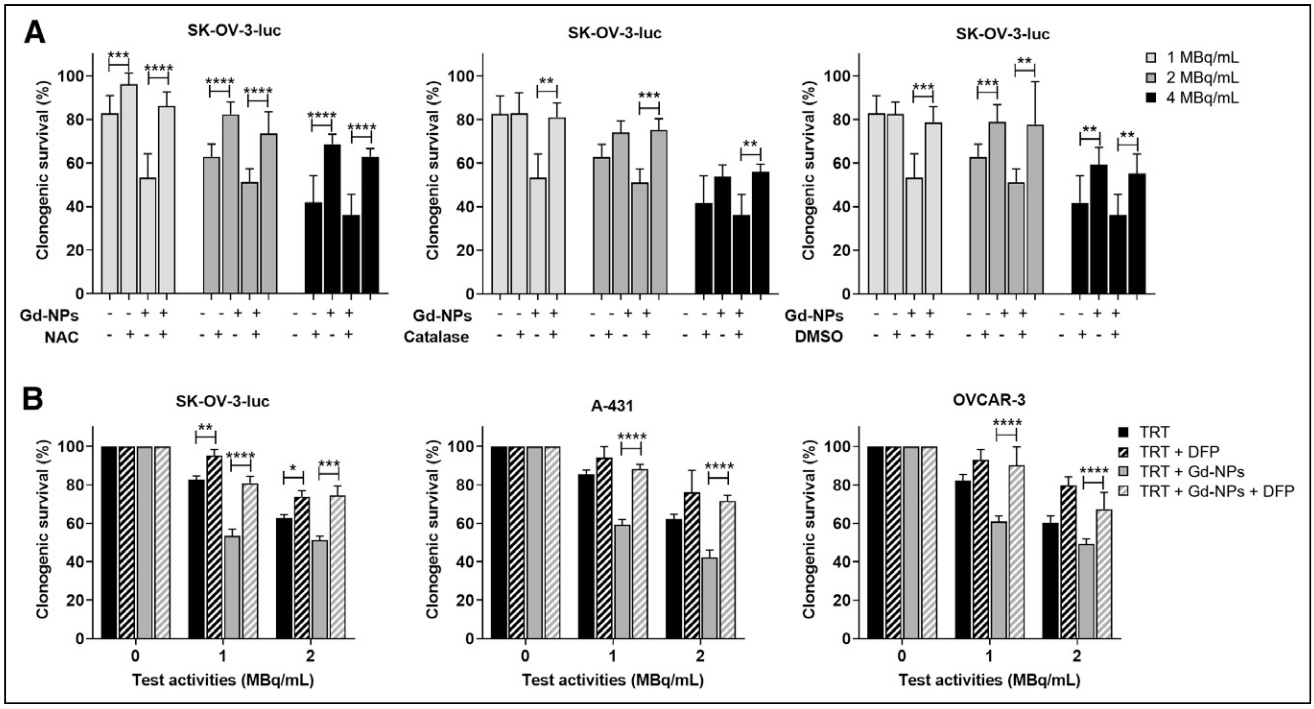

FIGURE 6. Oxidative stress is involved in radiosensitizing effects of Gd-NPs. (A) SK-OV-3-luc cells were incubated with [^{177}Lu]Lu-DOTA-trastuzumab, 1 MBq/mL, for 18 h with or without Gd-NPs, 10 mg/mL, with or without *N*-acetyl-L-cysteine (NAC), catalase, or dimethyl sulfoxide. Then, clonogenic survival was measured. (B) Clonogenic survival of SK-OV-3-luc, A-431, and OVCAR-3 cells incubated with [^{177}Lu]Lu-DOTA-trastuzumab (0–4 MBq/mL) with or without Gd-NPs, 10 mg/mL, for 18 h in presence or not of DFP. Results are mean ± SD of 3 independent experiments performed in triplicate. $^{*}P < 0.05$. $^{**}P < 0.01$. $^{***}P < 0.001$. $^{****}P < 0.0001$. DFP = deferiprone; DMSO = dimethyl sulfoxide; NAC = *N*-acetyl-L-cysteine; ns = not significant (Mann–Whitney *t* test) compared with cells treated with [^{177}Lu]Lu-DOTA-trastuzumab.

Moreover, using the relative tumor volume criteria, 5 of 8 mice in the group receiving 5 MBq of [^{177}Lu]Lu-DOTA-trastuzumab plus Gd-NP had an objective response (vs. 1/8 for 5 MBq of [^{177}Lu]Lu-DOTA-trastuzumab), 3 of 8 had stable disease (vs. 4/8), and 0 of 8 had progressive disease (vs. 3/8). In mice that received 10 MBq of [^{177}Lu]Lu-DOTA-trastuzumab (optimal activity study, Supplemental Table 1), 5 of 9 showed an objective response, 1 of 9 stable disease, and 3 of 9 progressive disease. These results highlight that besides improving efficacy, Gd-NPs allow TRT injected activities to be reduced.

Regimen 3 corresponded to the highest mass of Gd-NPs per injection and per day, suggesting that the synergistic effect with irradiation is proportional to the injected mass. This is also observed with EBRT in patients receiving large Gd-NPs masses (100 mg/kg 3 times) (NCT03818386). Moreover, in regimen 3, Gd-NPs were already injected at 24 h after the radiolabeled

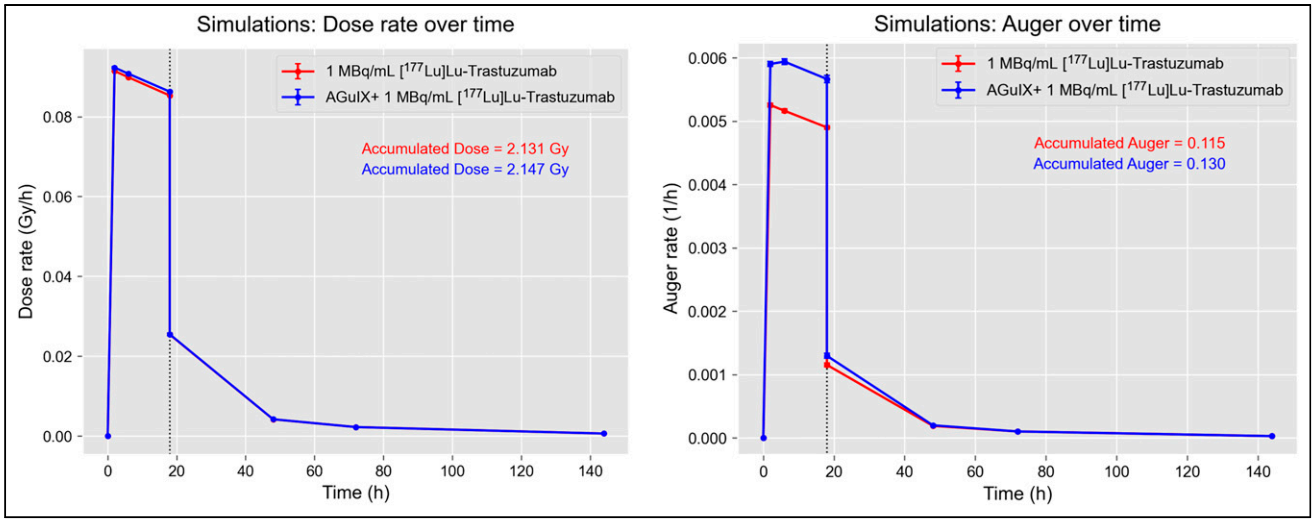

FIGURE 7. Physical aspects of TRT combined with Gd-NPs. Dose rate and accumulated dose in lysosomes at various time points for incubation and post-incubation scenarios (left). Auger electron production rate and cumulative number in lysosomes under same conditions as described for left panel (right).

antibody. The TRT enhancement potential of Gd-NPs might be further increased by conjugating the antibody to Gd-NPs. This approach could be interesting only if enough Gd-NPs can be delivered into tumors without loss of immunoreactivity. This would also require scaling up the synthesis of Gd-NPs-antibody conjugates in view of clinical translation. Moreover, it is interesting that the mean absorbed doses in tumor and normal tissues due to [^{177}Lu]Lu-trastuzumab (5 MBq) confirmed that irradiation of blood was at least 4 times lower than that of tumors (1.99 ± 0.21 Gy). The mean absorbed doses in other healthy tissues were even lower. Therefore, the radiosensitizing effect of Gd-NPs in healthy tissues should be limited.

Because Gd-NPs colocalized with lysosomes, Monte Carlo simulations were used to investigate the interaction between the decay spectra of ^{177}Lu and Gd-NPs in this subcellular compartment. The results indicated that Gd-NPs did not increase the cumulated ^{177}Lu dose delivered to lysosomes, thus excluding any dose enhancement effect. Moreover, the contribution of photoelectrons was extremely low, whereas the main difference concerned Auger electron production (+13% in the presence of Gd-NPs compared with ^{177}Lu alone). So far, only this increase (although rather modest from a quantitative point of view) could explain the radiosensitizing effect of Gd-NPs. However, in the absence of NPs, Auger electrons are generated homogeneously across the lysosome after the ionization of water molecules. Conversely, in the presence of Gd-NPs, Auger electrons are generated mostly at gadolinium atoms, leading to a very localized energy deposit around the NPs. These spurs of Auger electrons could have a different biologic significance and seem to cause lysosome disruption and production of iron-mediated reactive oxygen species leading to cell death (unpublished data, October 2023). These mechanisms and the qualitative nature of these Auger electrons are being investigated.

CONCLUSION

For the first time, to our knowledge, we demonstrated that combining TRT with Gd-NPs leads to radiosensitization and enhanced therapeutic efficacy while reducing the total injected activity. These findings could have a major impact on patients by reducing potential radiation-induced toxicities. This therapeutic combination represents an attractive solution for adjuvant TRT in the operating room to eliminate residual microscopic disease after cytoreductive surgery. Because Gd-NPs are already combined with EBRT in the clinic, the present study opens perspectives for the clinical translation of their combination with TRT. In this context, it would be interesting to consider also intravenous injection because indwelling catheters used for intraperitoneal administration can become infected, leading to peritonitis, a cause of multicycle chemoradiotherapy arrest in clinical trials on peritoneal metastases.

DISCLOSURE

This work was supported by a SIRIC Montpellier Cancer grant (INCa_Inserm_DGOS_12553), Fondation ARC pour la Recherche sur le Cancer (ARCPJA32020060002266), LabEx MabImprove, and région Occitanie. Léna Carmes is an employee of NH TherAguix. François Lux and Olivier Tillement possess shares of NH TherAguix. François Lux and Olivier Tillement have filed patent WO2011135101, which describes Gd-NPs used in this paper. Clara Diaz Garcia-Prada, Léna Carmes, Olivier Tillement, François Lux, Julie Constanzo, and Jean-Pierre Pouget have filed patent EP22306057, which describes the combination of Gd-NPs with TRT. No other potential conflict of interest relevant to this article was reported.

ACKNOWLEDGMENT

We thank Alexandre Pichard, Malick Bio Idrissou, and Yann Dromard for technical support.

KEY POINTS

QUESTION: Can Gd-NPs potentiate the effect of targeted TRT?

PERTINENT FINDINGS: Gd-NPs allow reducing the injected activity and improving the TRT therapeutic index through Auger electron emission.

IMPLICATIONS FOR PATIENT CARE: The Gd-NP–and–TRT combination is an attractive new therapeutic approach for patients with diffuse cancer disease, such as ovarian PC, to be used directly in the operating room after cytoreductive surgery.

REFERENCES

1. Key Statistics for ovarian cancer. American Cancer Society website. https://www.cancer.org/cancer/ovarian-cancer/about/key-statistics.html. Revised January 12, 2023. Accessed September 11, 2023.
2. Ledermann JA, Raja FA, Fotopoulou C, Gonzalez-Martin A, Colombo N, Sessa C. Newly diagnosed and relapsed epithelial ovarian carcinoma: ESMO clinical practice guidelines for diagnosis, treatment and follow-up. *Ann Oncol.* 2013;24:vi24–vi32.
3. Armstrong DK, Alvarez RD, Bakkum-Gamez JN, et al. Ovarian cancer, version 2.2020, NCCN clinical practice guidelines in oncology. *J Natl Compr Canc Netw.* 2021;19:191–226.
4. Moore K, Colombo N, Scambia G, et al. Maintenance olaparib in patients with newly diagnosed advanced ovarian cancer. *N Engl J Med.* 2018;379:2495–2505.
5. Oza AM, Cook AD, Pfisterer J, et al. Standard chemotherapy with or without bevacizumab for women with newly diagnosed ovarian cancer (ICON7): overall survival results of a phase 3 randomised trial. *Lancet Oncol.* 2015;16:928–936.
6. Ray-Coquard I, Pautier P, Pignata S, et al. Olaparib plus bevacizumab as first-line maintenance in ovarian cancer. *N Engl J Med.* 2019;381:2416–2428.
7. Foo T, George A, Banerjee S. PARP inhibitors in ovarian cancer: an overview of the practice-changing trials. *Genes Chromosomes Cancer.* 2021;60:385–397.
8. Estupina P, Fontayne A, Barret J-M, et al. The anti-tumor efficacy of 3C23K, a glyco-engineered humanized anti-MISRII antibody, in an ovarian cancer model is mainly mediated by engagement of immune effector cells. *Oncotarget.* 2017;8:37061–37079.
9. Kersual N, Garambois V, Chardès T, et al. The human Müllerian inhibiting substance type II receptor as immunotherapy target for ovarian cancer. *MAbs.* 2014;6:1314–1326.
10. Pouget J-P, Lozza C, Deshayes E, Boudousq V, Navarro-Teulon I. Introduction to radiobiology of targeted radionuclide therapy. *Front Med (Lausanne).* 2015;2:12.
11. Pouget J-P, Constanzo J. Revisiting the radiobiology of targeted alpha therapy. *Front Med (Lausanne).* 2021;8:692436.
12. Müller C, Zhernosekov K, Köster U, et al. A unique matched quadruplet of terbium radioisotopes for PET and SPECT and for α- and β^--radionuclide therapy: an in vivo proof-of-concept study with a new receptor-targeted folate derivative. *J Nucl Med.* 2012;53:1951–1959.
13. Seidl C, Zöckler C, Beck R, Quintanilla-Martinez L, Bruchertseifer F, Senekowitsch-Schmidtke R. ^{177}Lu-immunotherapy of experimental peritoneal carcinomatosis shows comparable effectiveness to ^{213}Bi-immunotherapy, but causes toxicity not observed with ^{213}Bi. *Eur J Nucl Med Mol Imaging.* 2011;38:312–322.
14. Zacchetti A, Martin F, Luison E, et al. Antitumor effects of a human dimeric antibody fragment ^{131} I-AFRA-DFM5.3 in a mouse model for ovarian cancer. *J Nucl Med.* 2011;52:1938–1946.
15. Persson HL, Kurz T, Eaton JW, Brunk UT. Radiation-induced cell death: importance of lysosomal destabilization. *Biochem J.* 2005;389:877–884.
16. Ray GL, Baidoo KE, Keller LMM, Albert PS, Brechbiel MW, Milenic DE. Preclinical assessment of ^{177}Lu-labeled trastuzumab targeting HER2 for treatment and management of cancer patients with disseminated intraperitoneal disease. *Pharmaceuticals (Basel).* 2011;5:1–15.

17. Hindié E, Zanotti-Fregonara P, Quinto MA, Morgat C, Champion C. Dose deposits from ^{90}Y, ^{177}Lu, ^{111}In, and ^{161}Tb in micrometastases of various sizes: implications for radiopharmaceutical therapy. *J Nucl Med.* 2016;57:759–764.
18. Gustafsson-Lutz A, Bäck T, Aneheim E, et al. Therapeutic efficacy of α-radioimmunotherapy with different activity levels of the ^{213}Bi-labeled monoclonal antibody MX35 in an ovarian cancer model. *EJNMMI Res.* 2017;7:38.
19. Bäck T, Chouin N, Lindegren S, et al. Cure of Human Ovarian Carcinoma Solid Xenografts by Fractionated α-Radioimmunotherapy with ^{211}At-MX35-F(ab′)2: influence of absorbed tumor dose and effect on long-term survival. *J Nucl Med.* 2017;58:598–604.
20. Deshayes E, Ladjohounlou R, Le Fur P, et al. Radiolabeled antibodies against Müllerian-inhibiting substance receptor, type II: new tools for a theranostic approach in ovarian cancer. *J Nucl Med.* 2018;59:1234–1242.
21. Boudousq V, Ricaud S, Garambois V, et al. Brief intraperitoneal radioimmunotherapy of small peritoneal carcinomatosis using high activities of noninternalizing ^{125}I-labeled monoclonal antibodies. *J Nucl Med.* 2010;51:1748–1755.
22. Knogler K, Grünberg J, Zimmermann K, et al. Copper-67 radioimmunotherapy and growth inhibition by anti–L1-cell adhesion molecule monoclonal antibodies in a therapy model of ovarian cancer metastasis. *Clin Cancer Res.* 2007;13:603–611.
23. Verheijen RH, Massuger LF, Benigno BB, et al. Phase III trial of intraperitoneal therapy with yttrium-90-labeled HMFG1 murine monoclonal antibody in patients with epithelial ovarian cancer after a surgically defined complete remission. *J Clin Oncol.* 2006;24:571–578.
24. Epenetos AA, Munro AJ, Stewart S, et al. Antibody-guided irradiation of advanced ovarian cancer with intraperitoneally administered radiolabeled monoclonal antibodies. *J Clin Oncol.* 1987;5:1890–1899.
25. Meredith RF, Buchsbaum DJ, Alvarez RD, LoBuglio AF. Brief overview of preclinical and clinical studies in the development of intraperitoneal radioimmunotherapy for ovarian cancer. *Clin Cancer Res.* 2007;13:5643s–5645s.
26. Rosenblum MG, Verschraegen CF, Murray JL, et al. Phase I study of ^{90}Y-labeled B72.3 intraperitoneal administration in patients with ovarian cancer: effect of dose and EDTA coadministration on pharmacokinetics and toxicity. *Clin Cancer Res.* 1999;5:953–961.
27. Alvarez RD, Huh WK, Khazaeli MB, et al. A phase I study of combined modality ^{90}yttrium-CC49 intraperitoneal radioimmunotherapy for ovarian cancer. *Clin Cancer Res.* 2002;8:2806–2811.
28. Mahé MA, Fumoleau P, Fabbro M, et al. A phase II study of intraperitoneal radioimmunotherapy with iodine-131-labeled monoclonal antibody OC-125 in patients with residual ovarian carcinoma. *Clin Cancer Res.* 1999;5:3249s–3253s.
29. Navarro-Teulon I, Lozza C, Pèlegrin A, Vivès E, Pouget J-P. General overview of radioimmunotherapy of solid tumors. *Immunotherapy.* 2013;5:467–487.
30. Boudousq V, Bobyk L, Busson M, et al. Comparison between internalizing anti-HER2 mAbs and non-internalizing anti-CEA mAbs in alpha-radioimmunotherapy of small volume peritoneal carcinomatosis using ^{212}Pb. *PLoS One.* 2013;8:e69613.
31. Li RG, Napoli E, Jorstad IS, et al. Calcium carbonate microparticles as carriers of ^{224}Ra: impact of specific activity in mice with intraperitoneal ovarian cancer. *Curr Radiopharm.* 2021;14:145–153.
32. Leidermark E, Hallqvist A, Jacobsson L, et al. Estimating the risk for secondary cancer after targeted α-therapy with ^{211}At intraperitoneal radioimmunotherapy. *J Nucl Med.* 2023;64:165–172.
33. Minnix M, Li L, Yazaki PJ, et al. TAG-72–targeted α-radionuclide therapy of ovarian cancer using ^{225}Ac-labeled DOTAylated-huCC49 antibody. *J Nucl Med.* 2021;62:55–61.
34. Lux F, Tran VL, Thomas E, et al. AGuIX® from bench to bedside: transfer of an ultrasmall theranostic gadolinium-based nanoparticle to clinical medicine. *Br J Radiol.* 2019;92:20180365.
35. Verry C, Dufort S, Villa J, et al. Theranostic AGuIX nanoparticles as radiosensitizer: a phase I, dose-escalation study in patients with multiple brain metastases (NANO-RAD trial). *Radiother Oncol.* 2021;160:159–165.
36. Verry C, Dufort S, Lemasson B, et al. Targeting brain metastases with ultrasmall theranostic nanoparticles, a first-in-human trial from an MRI perspective. *Sci Adv.* 2020;6:eaay5279.
37. Milenic DE, Wong KJ, Baidoo KE, et al. Targeting HER2: a report on the in vitro and in vivo pre-clinical data supporting trastuzumab as a radioimmunoconjugate for clinical trials. *MAbs.* 2010;2:550–564.
38. Repetto-Llamazares AHV, Larsen RH, Giusti AM, et al. ^{177}Lu-DOTA-HH1, a novel anti-CD37 radio-immunoconjugate: a study of toxicity in nude mice. *PLoS ONE.* 2014;9:e103070.
39. Pichard A, Marcatili S, Karam J, et al. The therapeutic effectiveness of ^{177}Lu-lilotomab in B-cell non-Hodgkin lymphoma involves modulation of G2/M cell cycle arrest. *Leukemia.* 2020;34:1315–1328.
40. Karam J, Constanzo J, Pichard A, et al. Rapid communication: insights into the role of extracellular vesicles during Auger radioimmunotherapy. *Int J Radiat Biol.* 2023;99:109–1118.
41. Rocchi P, Brichart-Vernos D, Lux F, et al. A new generation of ultrasmall nanoparticles inducing sensitization to irradiation and copper depletion to overcome radioresistant and invasive cancers. *Pharmaceutics.* 2022;14:814.
42. Constanzo J, Garcia-Prada CD, Pouget J-P. Clonogenic assay to measure bystander cytotoxicity of targeted alpha-particle therapy. *Methods Cell Biol.* 2023;174:137–149.
43. Naumann P, Liermann J, Fortunato F, et al. Sulforaphane enhances irradiation effects in terms of perturbed cell cycle progression and increased DNA damage in pancreatic cancer cells. *PLOS ONE*. 2017;12:e0180940.
44. Cunningham C, De Kock M, Engelbrecht M, Miles X, Slabbert J, Vandevoorde C. Radiosensitization effect of gold nanoparticles in proton therapy. *Front Public Health.* 2021;9:699822.
45. Bliss CI. The toxicity of poisons applied jointly. *Ann Appl Biol.* 1939;26:585–615.
46. Vaziri B, Wu H, Dhawan AP, Du P, Howell RW; SNMMI MIRD Committee. MIRD pamphlet no. 25: MIRDcell V2.0 software tool for dosimetric analysis of biologic response of multicellular populations. *J Nucl Med.* 2014;55:1557–1564.
47. Katugampola S, Wang J, Rosen A, Howell RW. MIRD pamphlet no. 27: MIRDcell V3, a revised software tool for multicellular dosimetry and bioeffect modeling. *J Nucl Med.* 2022;63:1441–1449.
48. Wong FC. MIRD: radionuclide data and decay schemes. *J Nucl Med.* 2009;50:2091.